

Lipopolysaccharide-Induced Preconditioning Attenuates Apoptosis and Differentially Regulates TLR4 and TLR7 Gene Expression after Ischemia in the Preterm Ovine Fetal Brain

Simerdeep K. Dhillon^{a, b} Alistair J. Gunn^b Yewon Jung^a Sam Mathai^b
Laura Bennet^b Mhoyra Fraser^{a, b}

^aLiggins Institute, and ^bDepartment of Physiology, University of Auckland, Auckland, New Zealand

Key Words

Preterm brain injury · Infection · Lipopolysaccharide · Hypoxia-ischemia · Preconditioning · Toll-like receptors · Cytokines

Abstract

Acute exposure to subclinical infection modulates subsequent hypoxia-ischemia (HI) injury in a time-dependent manner, likely by cross-talk through Toll-like receptors (TLRs), but the specific pathways are unclear in the preterm-equivalent brain. In the present study, we tested the hypothesis that repeated low-dose exposure to lipopolysaccharide (LPS) before acute ischemia would be associated with induction of specific TLRs that are potentially neuroprotective. Fetal sheep at 0.65 gestation (term is ~145 days) received intravenous boluses of low-dose LPS for 5 days (day 1, 50 ng/kg; days 2–5, 100 ng/kg) or the same volume of saline. Either 4 or 24 h after the last bolus of LPS, complete carotid occlusion was induced for 22 min. Five days after LPS, brains were collected. Pretreatment with LPS for 5 days decreased cellular apoptosis, microglial activation and reactive astrogliosis in response to HI injury induced 24 but not 4 h after the last dose of LPS. This was associated with upregulation of TLR4, TLR7 and IFN- β mRNA, and increased fetal plasma IFN- β con-

centrations. The association of reduced white matter apoptosis and astrogliosis after repeated low-dose LPS finishing 24 h but not 4 h before cerebral ischemia, with central and peripheral induction of IFN- β , suggests the possibility that IFN- β may be an important mediator of endogenous neuroprotection in the developing brain. © 2015 S. Karger AG, Basel

Introduction

Cerebral palsy is one of the most devastating consequences of hypoxia-ischemia (HI) before birth and is very common in preterm infants [1]. It is now recognized that the etiology of preterm brain injury is likely multifactorial. While HI is likely to be important, there is now compelling evidence that exposure to infection and secondary inflammation, both before and after birth, is highly associated with preterm brain injury and deficits in neuronal architecture and function in later life [2–9].

The clinical relationship between injury and infection is complex and closely intertwined with placental insufficiency [10–12]. This complexity is mirrored by preclinical evidence in the neonatal rat that single-dose exposure to lipopolysaccharide (LPS) can either protect or sensitize

to injury from other insults [13–17], depending on the time interval between exposure to infection and subsequent ischemia. Typically, single-dose administration of LPS 24 h before HI is neuroprotective, whereas LPS given 4 and 72 h before HI exacerbates injury [13, 18]. However, subacute clinical infection is also common and associated with adverse outcomes [19–21]. There is limited information on how such longer exposure to infection affects the response to later HI.

There is evidence that delayed preconditioning and sensitization are largely mediated by activation of members of the Toll-like receptor (TLR) family, which play a fundamental role in the initiation and activation of inflammatory responses to infectious and noninfectious stimuli [18, 22–25]. While studies in fetal and newborn animals have highlighted a strong relationship between the TLR4 ligand, LPS and brain injury [18, 24–26], very little is known regarding the involvement of other TLRs. Similarly, it is unclear whether specific TLR signaling may represent a secondary adaptation to attenuate immune responses following acute injury or conversely exacerbate underlying inflammatory responses that may lead to injury of the developing brain.

Studies in adult animal stroke models suggest that numerous preconditioning stimuli, including LPS, ultimately modulate TLR signaling and induce novel neuroprotective pathways [22, 27–31]. Systemic administration of the TLR9 ligand CpG oligodeoxynucleotide is neuroprotective against ischemic brain injury in stroke models through a similar mechanism to that of TLR4 which is dependent on tumor necrosis factor- α (TNF- α) [32, 33], whereas neuroprotection by treatment with the TLR7 ligand gardiquimod is associated with induction of type I interferons (IFNs) after ischemic brain injury [34]. Furthermore, in the mouse brain, TLR7 and TLR9 are the only TLRs that exhibit a developmental increase in mRNA expression throughout mid-embryogenesis and early postnatal stages [35] suggesting a greater role during development.

Based on these facts we tested the hypothesis that repeated exposure to a noninjurious, low dose of LPS before acute HI, induced by 22 min of reversible bilateral carotid occlusion in preterm fetal sheep at 0.65 gestation (term gestation \sim 145 days), would be associated with induction of TLR7 and/or TLR9 mRNA expression and other key inflammatory mediators within the fetal brain that are potentially neuroprotective. At this age, brain development is broadly equivalent to human brain development at 26–28 weeks gestation [36].

Cerebral ischemia was induced 4 and 24 h after the last dose of LPS, in view of evidence that vulnerability of the

developing brain to HI injury is dependent on the duration of the interval between LPS exposure and subsequent ischemia [18]. A simple model of acute carotid occlusion was used given the clinical importance of cerebral hypoperfusion in the pathogenesis of white matter injury [37–41]. This paradigm leads to diffuse white matter injury with no cystic or necrotic transformation on postmortem magnetic resonance imaging [42, 43], consistent with recent cohorts of preterm human infants [44–47].

Materials and Methods

Animals and Surgical Procedures

The University of Auckland Animal Ethics Committee approved the experimental procedures. Romney-Suffolk cross fetal sheep were instrumented at 89–90 days of gestation (gestation 0.65, term \sim 145 days gestation), equivalent to the human fetus of 28 weeks of gestation [36]. The general approach used was similar to that described previously [42, 43]. Briefly, ewes were anesthetized by an intravenous injection of propofol (5 mg/kg; Astra Zeneca Ltd., Auckland, New Zealand), and general anesthesia was maintained using 2–3% isoflurane in O₂. Ewes received 5 ml of streptocin (250,000 IU/ml procaine penicillin and 250 mg/ml dihydrostreptomycin; Stockguard Labs, Hamilton, New Zealand) intramuscularly for prophylaxis 30 min before the start of surgery. During surgery, maternal fluid balance was maintained with constant saline infusion, and the depth of anesthesia, maternal heart rate and respiration in the ewes were constantly monitored.

A maternal midline abdominal incision and uterotomy incision were performed to exteriorize the head, neck and forelimbs of the fetus. Polyvinyl catheters were placed into the right and left brachial arteries and veins of the fetus and amniotic sac. The vertebral-occipital anastomoses between the carotid arteries and vertebral arteries were ligated bilaterally to restrict blood supply to the carotid arteries. An inflatable silicone occluder (silicone tubing, Silclear, Degania Silicone, Degania Bet, Israel) was then placed around each carotid artery. Two pairs of electroencephalogram (EEG) electrodes (AS633-5SSF, Cooner Wire, Chatsworth, Calif., USA) were placed on the dura over the parasagittal parietal cortex (5 and 10 mm anterior to the bregma and 5 mm lateral) with a reference electrode placed over the occiput. Another pair of electrodes was placed over the dura, 5 mm lateral to the EEG electrodes to measure cortical impedance [42]. Electromyography was recorded to measure fetal body movement, by placing a pair of electrodes into the nuchal muscle. A pair of electrodes was placed on the chest to measure the fetal electrocardiogram. The head and forelimbs of the fetus were then returned to the uterus, and the incisions were closed. The leads for all the electrodes were exteriorized via the maternal flank, and polyvinyl catheters were placed in the maternal saphenous vein, to provide access for postoperative care and euthanasia.

Postoperative Care

Following surgery, the animals were kept in metabolic cages for the entire period of the study, and placed in 12-hour light and 12-hour dark cycles in a temperature-controlled room ($16 \pm 1^\circ\text{C}$, humidity $50 \pm 10\%$). Ewes were given water ad libitum and fed twice

daily between 9.00 and 16.00 h. A 5-day period of recovery was allowed before the start of experiments. Antibiotics were given daily; 600 mg i.v. Crystapen (benzylpenicillin sodium, Novartis, Auckland, New Zealand) for 4 days and 80 mg i.v. gentamicin (Pharmacia and Upjohn, Perth, Australia) for 3 days. Fetal vascular catheters were maintained patent by continuous infusion of heparinized saline (10 U/ml at a rate of 0.15–0.20 ml/h). Fetal and maternal arterial blood gases, pH and glucose/lactate levels were measured in whole blood (0.5 ml) collected daily in chilled heparin-lined syringes. Only fetuses whose arterial blood gases and lactate measurements were within the normal range ($PO_2 > 2.27$ kPa, pH > 7.32 ; lactate < 1.2 mmol/l) were included in the experiments. Fetal arterial blood samples (1.5 ml) were collected daily for measurement of cytokines and centrifuged at 4°C for 15 min (3,000 rpm) and stored at -80°C. The first (baseline) sample was collected 24 h before administration of saline or LPS boluses. On days 1–5 of administration of LPS or saline boluses, samples were collected at -30 min and 1, 4 and 8 h after each bolus LPS or saline, and then 1 h after occlusion and daily thereafter until postmortem assessment.

Experimental Design

Five days after surgery on day 94–95 of gestation, animals were randomly assigned to either control (n = 16) or treatment groups (n = 12). In the LPS groups, an intravenous bolus of LPS (derived from *Escherichia coli*, serotype 055:B5, Sigma-Aldrich, St. Louis, Mo., USA) was administered starting with a dose of 50 ng/kg of approximate weight (based on previous postmortem weights of fetuses on days 95–96 of gestation) of the fetus dissolved in 1 ml saline on day 1. For the following 4 days (days 2–5) a dose of 100 ng/kg was given. Animals then received either cerebral hypoperfusion induced by a 22-min period of bilateral carotid artery occlusion, 4 h after the last bolus of LPS (i.e. on day 5; 4 h LPS-OCCL group, n = 6) or ischemia induced 24 h after the last dose of LPS (i.e. on day 6; 24 h LPS-OCCL group, n = 6). In the saline control groups, 1 ml of saline vehicle was administered at the same times as in the LPS groups, and with either occlusion 4 h after the last bolus (4 h Sal-OCCL, n = 5), 24 h (24 h Sal-OCCL, n = 5) after the last bolus or no occlusion (Sal-CON, n = 6).

Successful occlusion was confirmed by a sustained fall in EEG intensity of 5 dB or more, with a fall in spectral edge of 4 Hz or more during occlusion as previously described [42]. Of the 22 animals occluded, occlusion failed in 3 fetuses. Thus, the final numbers of completed studies were for 4 h LPS-OCCL, n = 6, 4 h Sal-OCCL, n = 3, 24 h LPS-OCCL, n = 6, and 24 h Sal-OCCL, n = 4.

Postocclusion and Postmortem Assessments

Following occlusion or sham occlusion, the animals were monitored for a further 5 days and then killed by intravenous injection of an overdose of pentobarbital sodium (9 g, Pentobarb 300, Chemstock International, Christchurch, New Zealand) for postmortem examination on days 104–105 of gestation. Fetuses were weighed and sexed. Fetal brains were rapidly removed; one hemisphere was fixed in 4% paraformaldehyde in 0.1 M phosphate buffer, pH 7.4, for 1 week for histopathological studies, and the other hemisphere was slowly frozen on dry ice and then stored at -80°C for later molecular analysis.

Histology and Immunohistochemical Analysis

Brains collected postmortem were left for 1 week in fixative, then divided into 3 (A–C) coronal sections approximately 3–4 mm

in thickness; the anterior section (A) included the striatum and cortex; the middle section (B) included the thalamus, dorsal horn of the hippocampus and cortex, and the posterior section (C) included the thalamus, dorsal and ventral horn of the hippocampus and cortex. Sections were processed and paraffin embedded, then subsequently cut at 8- μ m thickness with a sledge microtome at the level of the midstriatum (26 mm anterior to stereotaxic zero) and midthalamus (17 mm anterior to the stereotaxic zero). Gross histopathological evaluation was conducted on thionin- and acid-fuchsin-stained sections by light microscopy with a Nikon Eclipse 80i microscope (Nikon Instruments Inc., Tokyo, Japan).

Oven-dried and xylene-deparaffinized sections were rehydrated in alcohol series and then washed with 0.1% PBS (phosphate-buffered saline). Antigen unmasking was performed using citrate buffer (pH 6.0) by the pressure cooking method (2100 retriever, Prestige Medical Ltd., Blackburn, UK). Endogenous peroxidase was quenched by treating the sections with 1% H_2O_2 in methanol for 30 min in darkness. Blocking was performed with 5% goat/horse serum in PBS for 1 h at room temperature. Washed slides were then incubated with corresponding primary and secondary antibodies overnight at 4°C.

The following primary antibodies were used: reactive microglia were labeled with goat anti-ionized calcium binding adapter molecule-1 antibody (1:200, Iba-1, Abcam, Cambridge, UK), reactive astrocytes were labeled with mouse anti-gial fibrillary acidic protein (1:500, GFAP, Chemicon International Inc., Temecula, Calif., USA), cells undergoing apoptosis were labeled with rabbit anti-cleaved caspase-3 ASP175 (1:200, Cell Signaling Technology, Danvers, Mass., USA), immature/mature oligodendrocytes were labeled with mouse monoclonal anti-2',3'-cyclic nucleotide 3'-phosphodiesterase (1:200, CNPase, Chemicon International Inc.). Rabbit anti-oligodendrocyte transcription factor-2 (1:200, Olig-2, Chemicon International Inc.) was used as a marker of all cells in the oligodendrocyte lineage [48]. Neuronal nuclei were labeled with monoclonal mouse anti-NeuN (1:200, Merck Millipore, Temecula, Calif., USA).

After overnight incubation with corresponding secondary antibodies (1:200), slides were repeatedly washed in PBS, then incubated with ExtrAvidin (Sigma-Aldrich) for 3 h at room temperature. Sections were then treated with SIGMAFAST™ 3,3'-diaminobenzidine (Sigma-Aldrich) to visualize immunoreactivity and permanently mounted with distyrene plasticizer xylene (Sigma-Aldrich). Negative controls were run in parallel.

Immunopositive cells were quantified under a Nikon Eclipse 80i microscope with a motorized stage and stereo investigator software V10 (MBF Bioscience, Williston, Vt., USA). Counting and estimation of the immunopositive cell density were done by an experimenter blinded to the studies. Sampling was performed using stereological principles. The area of interest was traced at $\times 2$ magnification and then translated onto a grid on the section at $\times 40$ magnification. A fractionator probe consisting of a counting frame for object inclusion and exclusion was then applied. The grid size was 500 \times 500 μ m, and the counting frame size was 100 \times 100 μ m. Immunopositive cell counts for each region were later converted to density (cells/mm²) by the equation: [estimated total counts by fractionator/contour area (μ m²)] $\times 10^6$. Photomicrographs were imaged at $\times 40$ and $\times 60$ magnification.

Numbers of activated microglia, reactive astroglia, activated caspase-3-positive cells and oligodendrocytes were quantified in the periventricular white matter (PVWM, coronal section A;

Fig. 1. Photomicrographs depicting areas of the coronal section at 26 and 17 mm anterior to stereotaxic zero used for immunohistochemical analysis. Cells positive for Olig-2 (which labels all cells in the oligodendrocyte lineage), CNPase (immature/mature oligodendrocytes), GFAP (reactive astrocytes), Iba-1 (activated microglia) and cleaved caspase-3 (apoptosis) were counted in the PVWM area (**a**; coronal section A), and NeuN-positive cells were counted in two regions (1 and 2) of the parasagittal cortex (**b**; coronal section B).

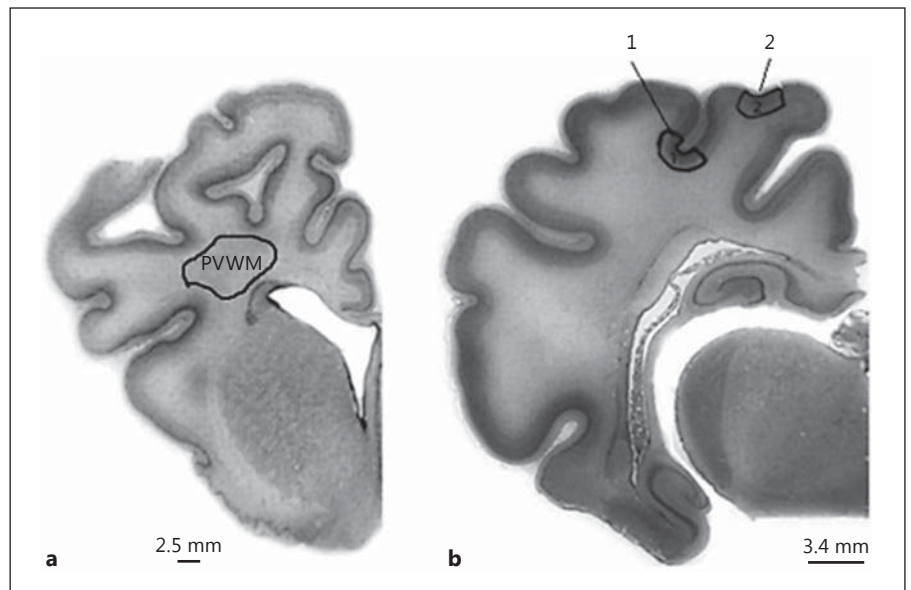


fig. 1a) across 1 hemisphere for each animal from 2 sections and counts averaged. In addition, neuronal survival was assessed in 2 representative regions of the parasagittal cortex (coronal section B; fig. 1b) from 1 hemisphere for each animal from 2 sections and counts averaged. Microglial activation was determined from numbers of Iba-1-labeled cells showing an amoeboid morphology with no cell processes. Reactive astrogliosis was assessed by the number of GFAP-labeled cells displaying hypertrophic cell bodies and cytoplasmic processes. Apoptosis was assessed by numbers of activated (cleaved) caspase-3-positive cells exhibiting chromatin condensation and nuclear fragmentation.

TLR7 Immunofluorescence

Immunofluorescence analysis was performed to determine the presence of TLR7 within the PVWM of paraffin-embedded brain sections from Sal-CON, 4 h LPS-OCCL, 4 h Sal-OCCL, 24 h LPS-OCCL and 24 h Sal-OCCL groups. Tissue sections (8- μ m thickness) were rehydrated as described above. Antigen unmasking was performed using tris(hydroxymethyl)aminomethane (Tris)-ethylenediaminetetraacetic acid (EDTA; pH 9.0) buffer, followed by treatment with 0.025% Triton X-100 to increase permeability. Blocking was performed using 10% normal goat serum in PBS. For TLR7 staining, tissue sections were incubated overnight at 4–8°C with rabbit anti-TLR7 antibody (1:400, Abcam) and subsequently incubated overnight at 4–8°C with fluorescent-labeled anti-rabbit secondary antibody (1:200, Alexa Fluor 488, Molecular Probes, Life Technologies, Carlsbad, Calif., USA). Nucleus counterstaining was performed using Hoechst 33258 nucleic acid stain (1:5,000, Molecular Probes, Life Technologies). In addition, staining in the absence of primary antibody was performed as negative controls. Image analysis was performed using an Olympus FluoView™ FV1000 confocal microscope (Olympus, Shinjuku, Tokyo, Japan).

Cryostat Sectioning and RNA Extraction

Frozen brains were sectioned at the level of the midstriatum (section A, as depicted in fig. 1a), using a cryostat (CM 3050S,

Leica Microsystems GmbH, Nussloch, Germany). Two whole coronal sections of 100 μ m were cut at this level for each sample, and these were added to 1 ml TRIzol reagent (Life Technologies), sonicated in ice-cold water and vortexed for 2–5 min, to ensure total homogenization of the tissue and then stored at –80°C. mRNA was extracted using the RNeasy Mini Kit (Qiagen, Valencia, Calif., USA), according to the manufacturer's instructions and stored at –80°C.

RNA Quantification and Integrity

The concentration and purity of the extracted RNA were confirmed by a Nanodrop ND-1000 spectrophotometer (Biosciences, Auckland, New Zealand). The integrity and size distribution of the RNA was determined by performing denaturing agarose gel electrophoresis and ethidium bromide staining. Briefly, RNA was electrophoresed in 1% formaldehyde agarose gel, which consisted of 1.25% of agarose in 1 \times 3-(N-morpholino)propanesulfonic acid (MOPS) buffer (20 mM MOPS, Free Acid; Santa Cruz Biotechnology Inc., Dallas, Tex., USA), 5 mM sodium acetate, 1 mM EDTA (pH 7.0), and ethidium bromide was added for staining RNA. RNA samples were prepared by diluting 5 μ g RNA samples with 5 g RNA loading dye [0.0016% v/v saturated bromophenol blue solution, 4 mM EDTA (pH 8.0), 0.89 M formaldehyde, 20% v/v glycerol, 31% deionized formamide and 4 \times MOPS]. Samples were then heated at 72°C for 5 min. Finally, samples were electrophoresed in 10 \times MOPS buffer at 90 V for 1.15 h. RNA samples suitable for downstream experiments were those that formed two clear bands (28S and 18S), and for which the intensity of the 28S band was approximately double that of the 18S band. Results of the gel electrophoresis are not shown.

cDNA Synthesis

First strand cDNA synthesis was performed using a SuperScript VILO™ cDNA Synthesis Kit (Invitrogen™, Life Technologies) according to the manufacturer's instructions. For each 20- μ l reaction, 1 μ g RNA, 4 μ l 5 \times VILO reaction mix, 2 μ l 10 \times superscript

Table 1. Primer sequences used in quantitative real-time PCR assays for target genes (SYBR green: TLR subtypes 2, 3, 4, 7 and 9, IRF3, IRF7, IFN- β ; TaqMan: TNF- α , IL-6 and IL-10)

Gene	Primer	Sequence (5'–3')	Accession No.	Amplicon size, bp
TLR2 (ovine)	Forward	GGCTGTAATCAGCGTGTTC	NM001048231	160
	Reverse	GATCTCGTTGTCCGACAGGT		
TLR3 (ovine)	Forward	TCAGCTCCAAGTGGAGAACC	NM001135928	150
	Reverse	CACCCAGGAGAGAAGTCTTTGA		
TLR4 (ovine)	Forward	TGGATTTATCCAGATGCGAAA	NM001135930	152
	Reverse	GGCCACCAGCTTCTGTAAAC		
TLR7 (ovine)	Forward	CTGGACCATCTGGTGGAGAT	NM001135059	154
	Reverse	GCTGGTTTTCCATCCAGGTAA		
TLR9 (ovine)	Forward	CCCTGGAGAAGCTGGACAT	NM001011555	175
	Reverse	GACAGGTCCACGAAGAGCAG		
IRF3 (ovine)	Forward	CCCTCACCTCGACCAGTAA	XM_004015378	66
	Reverse	GGGACACTGAATACCAGACACA		
IRF7 (ovine)	Forward	GGCAAGTGCAAAGTCTACTGG	XM_004019737	108
	Reverse	GAAGTCAAAGATGGGCGTGT		
IFN- β (ovine)	Forward	ACTCCTGGGGCAGTTACCTT	XM004023050	139
	Reverse	GTGCTGGAGCACCTCATAACA		
GAPDH (ovine)	Forward	GTCCGTTGTGGATCTGACCT	NM001190390	245
	Reverse	TGCTGTAGCCGAATTCATTG		
TNF- α (ovine)	Forward	GCCCTGGTACGAACCCATCT	NM001024860	112
	Reverse	CTGCCCAGACTCGGCATAGT		
	TaqMan probe	CAGTGCTGAGATCAACCT		
IL-6 (ovine)	Forward	CCTCCAGGAACCCAGCTATG	NM001009392	101
	Reverse	GGTAGGGAAAGCAGAAGTCATCA		
	TaqMan probe	ACTCCCTCTTCACAAGC		
IL-10 (ovine)	Forward	TGCCACAGGCTGAGAACCA	NM001009327	60
	Reverse	TCTCCCCCAGCGAGTTCA		
	TaqMan probe	CCTGACATCAAGGAGCA		
GAPDH (bovine)	Forward	TGCCGCCTGGAGAAACC	U85042	122
	Reverse	CCTCTGACGCCTGCTTCAC		
	TaqMan probe	CCAAGTATGATGAGATCAAGAA		
18s		4352930E	X03205	187

enzyme mix and nuclease-free water were added to 200 μ l polymerase chain reaction tubes (Axygen, Union City, Calif., USA). Reverse transcription reactions were performed at 25°C for 10 min, then at 42°C for 60 min and finally at 85°C for 5 min in a Mastercycler™ (Eppendorf, Hamburg, Germany) 96-well thermal cycler. The cDNA produced was stored at –20°C.

Primer Design, Determination of PCR Efficiency and Selection of Reference Genes

Primers for SYBR green-based detection of target genes, TLR subtypes 2, 3, 4, 7 and 9, interferon regulatory factors (IRF)3 and 7 and IFN- β (table 1), were ovine specific and were designed using

Oligoperfect Designer (Invitrogen, Life Technologies). Primer and probe sets for target genes (table 1), TNF- α , interleukins 6 (IL-6) and 10 (IL-10) were ovine specific and designed using the Primer Express software (Applied Biosystems, Foster City, Calif., USA). The specificity of the primers was tested using BLAST analysis against the NCBI database. Specificity of primers for SYBR green detection was also tested through qualitative PCR on cDNA. Briefly, PCR was performed using forward and reverse primers. The PCR cycle consisted of: 94°C for 3 min, followed by 40 cycles at 94°C for 30 s, 58°C for 1 min and 72°C for 1 min. The final extension was performed at 72°C for 5 min. Reactions were performed with a Mastercycler™ 96-well thermal cycler and PCR products

analyzed on a 1.5% agarose gel. DNA products were purified and sequenced (Allan Wilson Centre, Massey University, Palmerston North, New Zealand) and compared to the expected target sequence to ensure primer specificity.

Optimum cDNA and primer concentrations were determined prior to carrying out quantitative real-time PCR experiments. For SYBR green detection, the amplification efficiencies were estimated with standard curves using serial dilutions of the fetal spleen cDNA (50, 25, 10 and 5 $\mu\text{g}/\mu\text{l}$) and two primer concentrations (5 and 10 μM) for all genes of interest and calculated using the slope of a linear regression model, according to the equation: $E = 10(-1/\text{slope})$ [49]. The following 4 reference genes were selected for stability evaluation for SYBR green detection: glyceraldehyde 3-phosphate dehydrogenase (GAPDH), YWHAZ, SDHA and β -actin. Stability of expression among the housekeeping genes was assessed using the algorithm BestKeeper software application [50]; of the 4 putative housekeeping genes tested, GAPDH had the most stable level of expression. For TaqMan-based detection, 18S ribosomal RNA was chosen as the housekeeping gene since it was previously validated for use [51, 52].

Quantitative Real-Time PCR

TLRs 2, 3, 4, 7 and 9, IRF3, IRF7 and IFN- β transcript abundance was determined by quantitative real-time PCR using SYBR green (Invitrogen, Life Technologies)-based detection, whereas TNF- α , IL-6 and IL-10 were determined by TaqMan Gene Expression Assays (Applied Biosystems). For SYBR green-based detection, singleplex amplification was performed with a total volume of 10 μl , containing 5 μl fast SYBR green PCR Master Mix (Molecular Probes, Life Technologies), 1 μl cDNA template, 1 μl each of forward and reverse primers and 2 μl nuclease-free water (Ambion, Life Technologies, Auckland, New Zealand). For TaqMan-based detection, singleplex amplification was performed with a total reaction volume of 10 μl , containing 5 μl TaqMan Universal PCR Master Mix (Applied Biosystems), 1 μl cDNA template, 250 nM probe, 900 nM forward and reverse primers and 2.75 μl nuclease-free water (Ambion).

A positive control (cDNA obtained from LPS-treated fetal spleen or ovine cerebellum), nontemplate control and nonamplification control reactions were also included. The housekeeping gene, GAPDH (SYBR green) or 18S (TaqMan) was included in each plate to control for interplate variability. Amplification of gene transcripts was performed in triplicate on an ABI PRISM 7900HT sequence detector (Applied Biosystems). For SYBR green detection, the thermal profile of the reaction was: 95°C for 10 min, 40 cycles of denaturation and annealing/extension at 95°C for 1 s and 60°C for 30 s, respectively, followed by a dissociation curve at 95°C for 15 s, 60°C for 15 s and 95°C for 15 s. For TaqMan-based detection, the thermal profile of the reaction was: melt at 95°C for 15 s, anneal/extend for 40 cycles at 60°C for 1 min. Data were processed with the SDS v2.1 software (Applied Biosystems).

Analysis of gene expression was performed using the relative quantification method (ΔC_t method) [53]. The C_t value of the target gene was subtracted from the mean C_t value of the internal standard (housekeeping gene GAPDH or 18S) for the same sample to obtain a value for ΔC_t . $\Delta\Delta C_t$ was calculated by subtracting the ΔC_t value of target from the calibrator sample. The mean of the saline group C_t values was used as a calibrator sample. n -fold changes in mRNA expression of target genes relative to the housekeeping gene GAPDH or 18S were calculated by $2^{-\Delta\Delta C_t}$.

IFN- β , TNF- α , IL-6 and IL-10 Enzyme-Linked Immunosorbent Assays

IFN- β fetal plasma levels were determined using a commercially available ovine specific enzyme-linked immunosorbent assay (ELISA; BlueGene Biotech, Shanghai, China) according to the manufacturer's instructions. IFN- β ranged from 0 to 1,000 pg/ml with a detection sensitivity of 1.00 pg/ml. TNF- α , IL-6 and IL-10 concentrations were measured using in-house ELISAs. TNF- α was detected using antibodies specific to the ovine species (Epitope Technologies, Melbourne, Vic., Australia; Centre for Animal Biotechnology, University of Melbourne). Standards were ovine recombinant (Protein Express, Cincinnati, Ohio, USA). TNF- α ranged from 0 to 10 ng/ml with a detection sensitivity of 0.354 ng/ml. Internal quality controls were included in each assay. IL-6 was detected using antibodies specific to ovine IL-6 (Epitope Technologies). Standards were ovine recombinant IL-6 (Protein Express). The standard series ranged from 0 to 5 ng/ml. The assay sensitivity was 0.097 ng/ml and internal quality controls were included in each assay. IL-10 was detected using antibodies specific to the bovine species (AbD Serotec, MorphoSys, Kidlington, UK). Standards were recombinant bovine IL-10 (kindly provided by Prof. G. Entrican, Moredun Research Institute, Scotland) and ranged from 0 to 10 biological units/ml with a detection sensitivity of 0.086 biological units/ml [54, 55]. Internal quality controls were included in each assay.

Statistical Analysis

All quantitative data are presented as means \pm standard error of the mean (SEM). Statistical significance was accepted when $p < 0.05$. Changes in physiological variables (pH, blood gases, glucose and lactate) were assessed using repeated measures mixed-model analysis (SAS v9.4; SAS Institute, Cary, N.C., USA) with group and time as the factors as well as their interactions. Tukey's post hoc test was used to perform pairwise comparisons of all group means. Immunohistochemical and quantitative real-time PCR data were statistically analyzed using ANOVA with Tukey's post hoc test.

Results

Fetal Arterial Blood Gas and Metabolic Status

Baseline pH, blood gases, glucose and lactate were within normal physiological ranges and were not significantly different between groups (table 2). There was no significant interaction between group and time for arterial pH, PaCO₂, PaO₂, lactate and glucose. Pairwise comparisons between the two factors showed that plasma lactate concentrations changed significantly over time within the LPS group ($p < 0.05$), although post hoc, no specific time points were significantly different by the Tukey test. Due to sampling difficulty, data were not available during and immediately after occlusion.

Gross Histopathology

No overt histopathological damage was seen on thionin- and acid-fuchsin-stained coronal sections in the Sal-

CON group. Bilateral carotid artery occlusion for 22 min was associated with diffuse PVWM loss, with no cystic or necrotic transformation in any of the groups.

Activated Caspase-3 in the PVWM

There was a significant increase in expression of activated caspase-3 in the PVWM in both 4 h Sal-OCCL and 24 h SAL-OCCL groups ($p < 0.05$), and the 4 h LPS-OCCL group ($p < 0.05$; fig. 2a–e, 3a). Activated caspase-3 in the PVWM of the Sal-CON was below the level of detection. There was no significant difference in the number of caspase-3-positive cells within the PVWM between 4 h LPS-OCCL and 4 h Sal-OCCL groups. However, LPS pretreatment was associated with reduced caspase-3 expression in the PVWM in the 24 h LPS-OCCL group ($p < 0.05$).

Microglial Activation and Reactive Astrogliosis in the PVWM

Iba-1-positive cells were increased in the Sal-OCCL groups compared to Sal-CON, at both 4 h ($p < 0.05$) and 24 h ($p < 0.05$), and in the LPS-OCCL groups at both 4 h ($p < 0.05$) and 24 h ($p < 0.05$; fig. 2f–j, 3b). There was no significant difference in the number of Iba-1-positive cells between the 4 h LPS-OCCL and 4 h Sal-OCCL groups. However, in the 24 h LPS-OCCL group, it was significantly lower ($p < 0.05$) relative to its Sal-OCCL control.

Similarly, the number of GFAP-labeled reactive astrocytes was significantly increased ($p < 0.05$) within the PVWM in the 4 h LPS-OCCL and Sal-OCCL ($p < 0.05$) groups compared to Sal-CON (fig. 2k–o, 3c). In contrast, the number of GFAP-positive cells in the 24 h LPS-OCCL group was significantly lower ($p < 0.05$) compared to Sal-CON. Furthermore, GFAP expression was significantly lower ($p < 0.05$) in the 24 h LPS-OCCL group compared to its Sal-OCCL control and the 4 h LPS-OCCL group ($p < 0.05$).

Oligodendrocyte Cell Number

The number of Olig-2-positive cells within the PVWM was significantly greater in the 24 h Sal-OCCL group ($p < 0.05$) than in Sal-CON, and in the 4 h ($p < 0.05$) and 24 h LPS-OCCL compared to Sal-CON ($p < 0.05$, fig. 4a–e, 5a). No significant difference was observed between 4 and 24 h LPS-OCCL and Sal-OCCL groups (fig. 4a).

In contrast, CNPase expression in the LPS-OCCL and Sal-OCCL groups was not significantly different from Sal-CON (fig. 4f–j, 5b). In addition, there was no significant difference in the number of CNPase-positive cells between LPS-OCCL and Sal-OCCL groups at both 4 and

Table 2. Arterial pH, blood gases, glucose and lactate levels

	Day 1		Day 2			Day 3			Day 4			
	baseline	+1 h	+4 h	+8 h	-30 min	+1 h	+4 h	+8 h	-30 min	+1 h	+4 h	+8 h
<i>pH</i>												
Sal-OCCL	7.39±0.00	7.39±0.00	7.38±0.00	7.39±0.00	7.37±0.00	7.38±0.01	7.38±0.00	7.39±0.01	7.38±0.01	7.37±0.01	7.37±0.00	7.38±0.01
LPS-OCCL	7.36±0.01	7.36±0.02	7.34±0.01	7.35±0.01	7.37±0.00	7.37±0.01	7.35±0.01	7.37±0.01	7.36±0.00	7.36±0.00	7.35±0.01	7.36±0.01
<i>PaCO₂, mm Hg</i>												
Sal-OCCL	47.7±1.8	49.7±0.3	46.95±4.08	49.1±1.0	48.98±3.15	50.37±1.24	51.6±0.78	47.8±0.9	49.7±1.2	51.1±1.1	49.32±1.79	50.4±0.6
LPS-OCCL	51.38±1.58	50.98±1.35	52.76±3.19	53.96±1.80	53.89±3.39	48.84±1.12	55.33±1.40	51.06±1.20	50.19±1.25	49.6±1.4	48.52±2.47	50.00±3.04
<i>PaO₂, mm Hg</i>												
Sal-OCCL	26.6±0.1	25.5±1.3	26.53±0.77	26.6±1.1	25.14±0.75	26.1±0.1	25.55±1.08	25.08±1.21	25.73±0.86	25.43±0.63	26.16±0.66	25.77±0.78
LPS-OCCL	24.78±0.63	25.1±1.3	22.32±1.07	22.38±1.06	24.9±0.6	25.1±1.3	23.47±0.55	23.87±0.73	24.44±0.21	25.2±1.9	23.77±1.28	27.56±2.19
<i>Glucose, mmol/l</i>												
Sal-OCCL	0.74±0.16	0.98±0.10	0.79±0.11	0.73±0.13	0.59±0.15	0.87±0.09	0.76±0.15	0.86±0.13	0.76±0.08	0.73±0.19	0.66±0.16	0.83±0.16
LPS-OCCL	0.82±0.05	0.77±0.04	0.97±0.07	1.08±0.07	0.77±0.05	0.78±0.07	0.95±0.10	1.01±0.11	0.81±0.05	0.69±0.11	0.70±0.06	0.62±0.00
<i>Lactate, mmol/l</i>												
Sal-OCCL	1.00±0.35	1.31±0.40	0.93±0.26	0.94±0.20	0.80±0.18	1.135±0.12	0.91±0.15	1.87±0.83	1.15±0.07	1.00±0.17	0.81±0.24	1.17±0.19
LPS-OCCL	1.19±0.14	0.91±0.05	1.05±0.15	1.17±0.20	1.10±0.07	1.00±0.08	1.22±0.07	1.24±0.09	1.19±0.08	1.13±0.03	1.03±0.07	1.26±0.10

Fetal physiological parameters (arterial pH, blood gases, glucose and lactate values) on days 1–4 and 24 h after occlusion (day +1) in both Sal-OCCL (4 h, n = 4; 24 h, n = 6) and LPS-OCCL (4 h, n = 6; 24 h, n = 3) groups. The LPS-OCCL group received intravenous bolus injections of LPS dissolved in 1 ml saline: day 1 = 50 ng/kg and days 2–5 = 100 ng/kg of LPS. The Sal-OCCL group received 1 ml saline. Bilateral carotid occlusion (22 min) was performed on either day 5, 4 h after completion of the final LPS administration, or on day 6, 24 h after completion of the final LPS administration. Data are presented as means ± SEM.

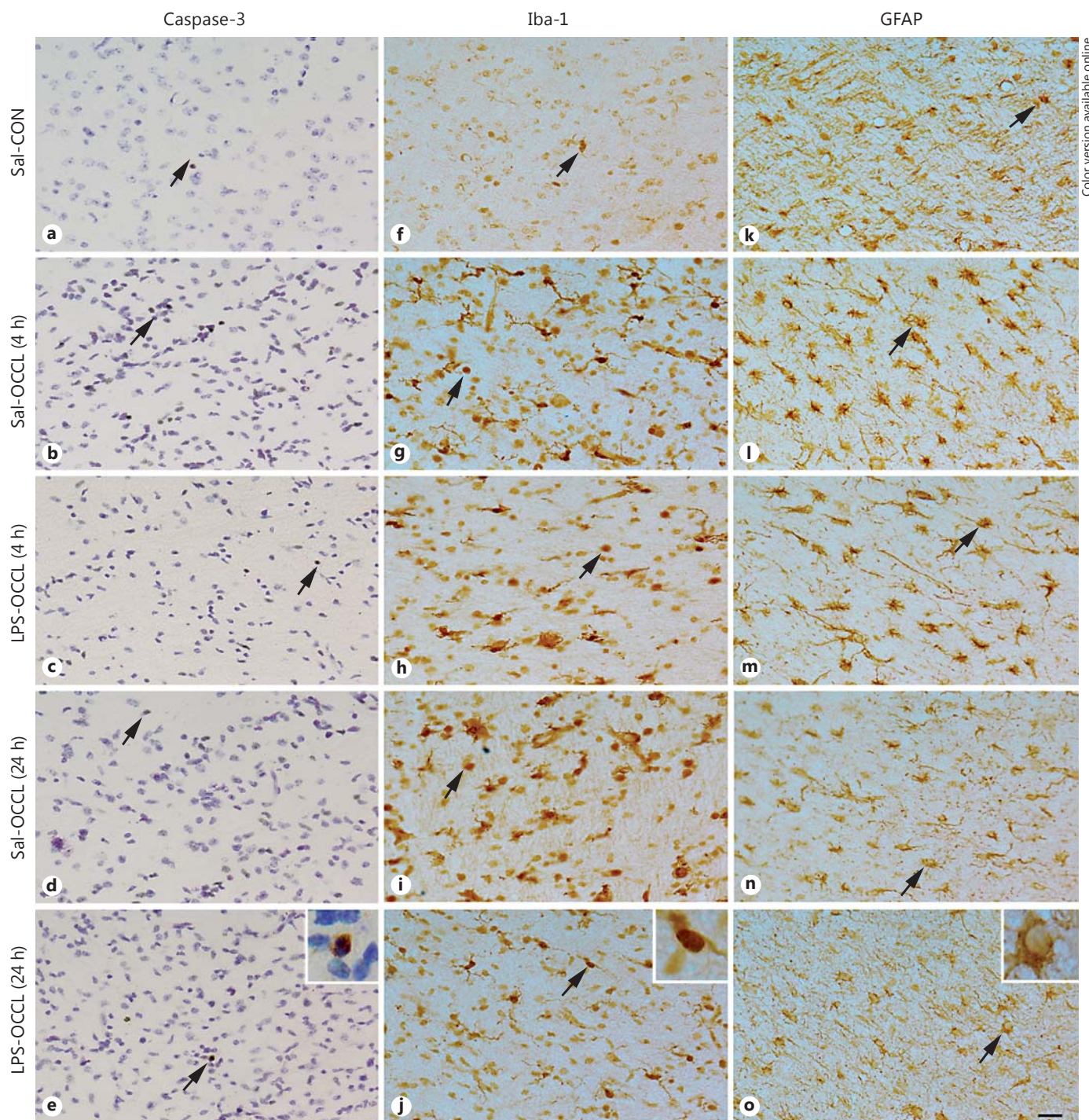


Fig. 2. Representative photomicrographs of activated caspase-3, Iba-1 and GFAP in the PVWM. The arrows point to representative cells within each photo. Saline sham occlusion control = Sal-CON (n = 4; **a, f, k**), occlusion 4 h after saline = 4 h Sal-OCCL (n = 3; **b, g, l**), occlusion 4 h after LPS = 4 h LPS-OCCL (n = 6; **c, h, m**), oc-

clusion 24 h after saline = 24 h Sal-OCCL (n = 4; **d, i, n**), occlusion 24 h after LPS = 24 h LPS-OCCL (n = 6; **e, j, o**). Magnification $\times 40$, scale bar = 20 μm for all photomicrographs. **Insets** Higher-magnification images ($\times 60$) of cells indicated by arrows.

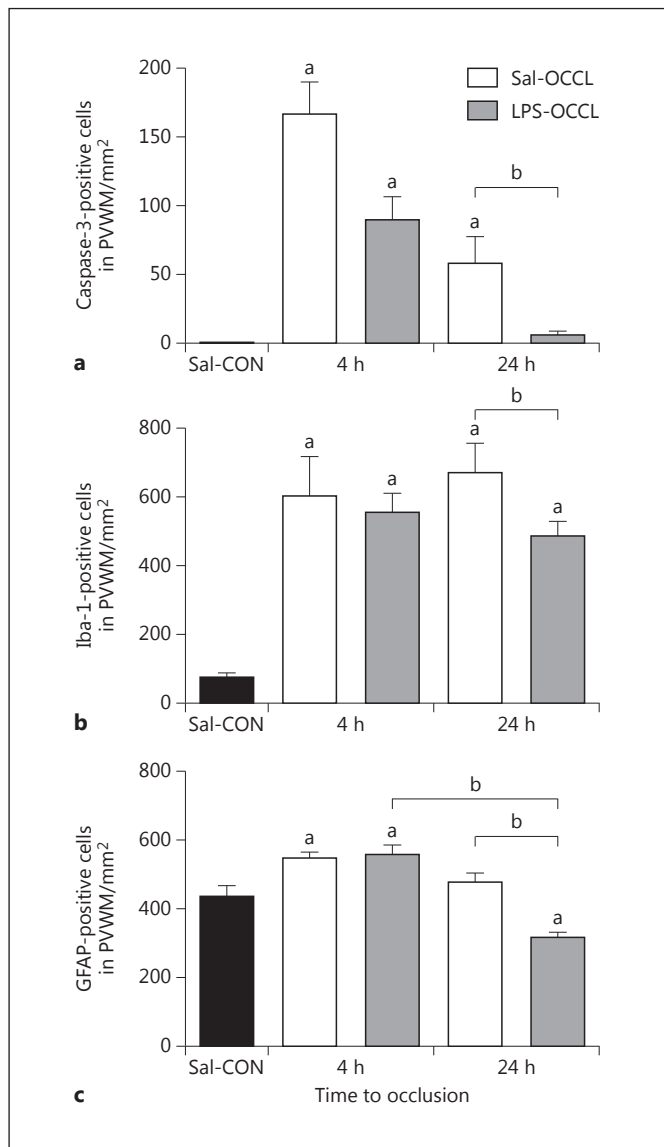


Fig. 3. Number of activated caspase-3- (a), Iba-1- (b) and GFAP-positive (c) cells in the PVWM. Cell numbers are presented as means \pm SEM. Saline sham occlusion control = Sal-CON (n = 4), occlusion 4 h after saline = 4 h Sal-OCCL (n = 3), occlusion 4 h after LPS = 4 h LPS-OCCL (n = 6), occlusion 24 h after saline = 24 h Sal-OCCL (n = 4), occlusion 24 h after LPS = 24 h LPS-OCCL (n = 6). ^a p < 0.05: significant difference from Sal-OCCL; ^b p < 0.05: significant difference between other groups.

24 h. However, significantly more CNPase-positive cells were seen (p < 0.05) in the 24 h LPS-OCCL group than the 4 h LPS-OCCL group. Furthermore, differences in the morphology of CNPase-positive cells were seen between groups (fig. 4f–j). In the Sal-OCCL groups, the cells had fewer and stunted processes, while extended and dense

processes were seen on CNPase-positive cells in the 24 h LPS-OCCL group. No difference was observed between the morphological characteristics of 4 h LPS-OCCL and Sal-OCCL groups.

Cortical Neuronal Density

The mean number of intact NeuN-positive cells in the parasagittal cortex in the LPS-OCCL and Sal-OCCL groups was not significantly different from Sal-CON (fig. 4k–o, 5c). There was no significant difference in the number of NeuN-positive cells between the 4 and 24 h LPS-OCCL and Sal-OCCL groups. Cortical expression of NeuN was significantly greater (p < 0.05) in the 24 h LPS-OCCL group compared with the 4 h LPS-OCCL group.

Differential Regulation of TLR mRNA Expression after HI Injury in the LPS-Pretreated Brain

TLR4 mRNA expression in the 24 h LPS-OCCL group was significantly greater (p < 0.05) than in Sal-OCCL (fig. 6a), whereas the 4 h LPS-OCCL group was not significantly different from its Sal-OCCL control. There was a significant increase (p < 0.05) in TLR7 mRNA expression in the 24 h LPS-OCCL group compared to Sal-OCCL (fig. 6b). However, there was no significant difference in TLR7 mRNA expression between LPS-OCCL and Sal-OCCL groups when occlusion was performed 4 h after the last dose of LPS.

There was no statistical difference in TLR9, TLR3 and TLR2 mRNA expression between either LPS-OCCL and Sal-OCCL groups (fig. 6c–e). However, there was a non-significant trend toward lower levels in TLR9 mRNA expression in the 24 h LPS-OCCL group, compared to Sal-OCCL, and similarly in the 24 h LPS-OCCL group compared to the 4 h LPS-OCCL group.

IRF3 and IRF7 mRNA Expression

Since upregulation of IFN- β expression could be the result of TLR4 and/or TLR7 signaling regulation, further expression studies were undertaken to determine which TLR signaling pathway was involved. There were no significant differences in IRF3 and IRF7 mRNA expression between the LPS-OCCL and Sal-OCCL groups (fig. 6f, g).

Upregulation of IFN- β mRNA Expression after HI Injury in the LPS-Pretreated Brain

IFN- β expression was significantly upregulated (p < 0.05) in the 24 h LPS-OCCL group compared to Sal-OCCL, whereas there was no significant difference between 4 h LPS-OCCL and Sal-OCCL groups (fig. 7a).

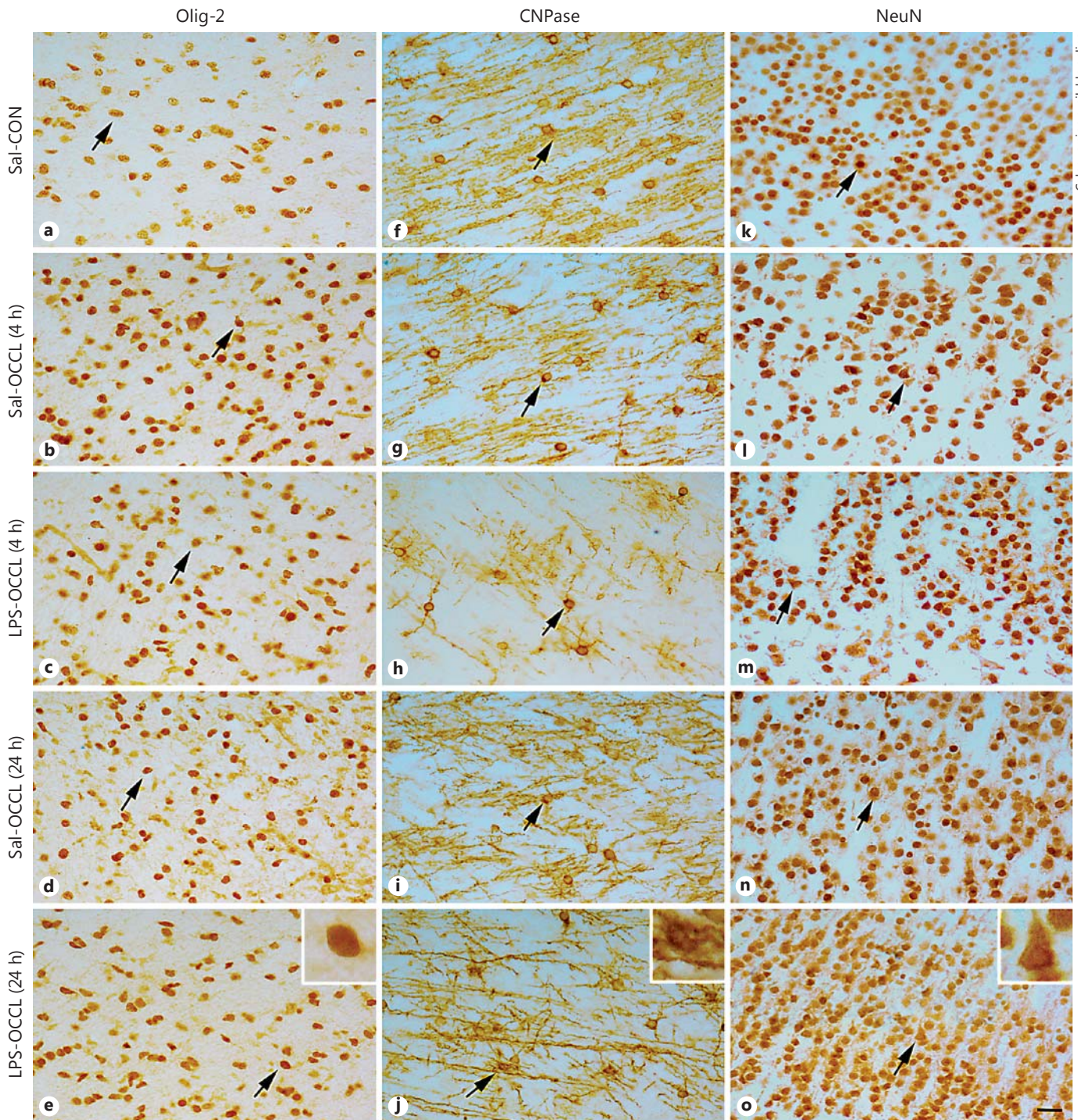


Fig. 4. Representative photomicrographs of Olig-2 and CNPase in the PVWM, and NeuN in the parasagittal cortex. The arrows point to representative cells within each photo. Saline sham occlusion control = Sal-CON (n = 4; **a, f, k**), occlusion 4 h after saline = 4 h Sal-OCCL (n = 3; **b, g, l**), occlusion 4 h after LPS = 4 h LPS-OCCL

(n = 6; **c, h, m**), occlusion 24 h after saline = 24 h Sal-OCCL (n = 4; **d, i, n**), occlusion 24 h after LPS = 24 h LPS-OCCL (n = 6; **e, j, o**). Magnification $\times 40$, scale bar = 20 μm for all photomicrographs. **Insets** Higher-magnification images ($\times 60$) of cells indicated by arrows.

TNF- α , IL-6 and IL-10 mRNA Expression

There was no statistical difference in expression of TNF- α , IL-6 or IL-10 mRNA between the LPS-OCCL and Sal-OCCL groups (fig. 7b–d).

Expression of TLR7 Protein in the PVWM

TLR7-positive cells were mostly confined to cells in the PVWM and cortical regions of the brain. Within the PVWM, TLR7-positive cells looked morphologically similar to microglia, astrocytes or oligodendrocytes (fig. 8). Intensity of staining appeared to be lower in the Sal-CON, 4 h Sal-OCCL, 4 h LPS-OCCL and 24 h Sal-OCCL groups and was confined to the perinuclear region with some granular cytoplasmic staining. By contrast, TLR7 immunostaining appeared to be more intense and was predominantly perinuclear in nature in the 24 h LPS-OCCL group.

LPS Preconditioning Triggers a Robust Fetal Plasma IFN- β Response to HI

Plasma samples were available for the 24 h LPS-OCCL and 24 h Sal-OCCL cohort of animals only. Plasma measurements of IFN- β in the 24 h LPS-OCCL group 5 days after carotid occlusion were above the upper limit of the calibration range (1,000 pg/ml) and were greater than in the Sal-OCCL group ($p < 0.05$, 24 h LPS-OCCL $1,000.0 \pm 0.0$ pg/ml, $n = 5$; 24 h Sal-OCCL 177.2 ± 59.8 , $n = 4$ pg/ml; fig. 9a). There were no significant differences in plasma concentrations of TNF- α , IL-6 or IL-10 between groups (fig. 9b–d). Furthermore, IL-6 concentrations were all below the level of detection (0.097 ng/ml) for the 24 h LPS-OCCL group.

Discussion

The present study demonstrates that in preterm fetal sheep, repeated low-dose, noninjurious exposure to LPS over 5 days, with the last dose given 24 h but not 4 h before cerebral ischemia, attenuates the inflammatory and astroglial reaction and reduces apoptosis within the PVWM after 5 days of recovery. These findings are consistent with previous evidence in the neonatal rat that a single acute exposure to LPS 24 h before HI injury typically induces preconditioning [18]. We show for the first time that this preconditioning effect was associated with upregulation of mRNA for TLR4, TLR7 and IFN- β , and a considerable increase in plasma IFN- β levels, suggesting the possibility that IFN- β may be an important mediator of endogenous neuroprotection. These findings have po-

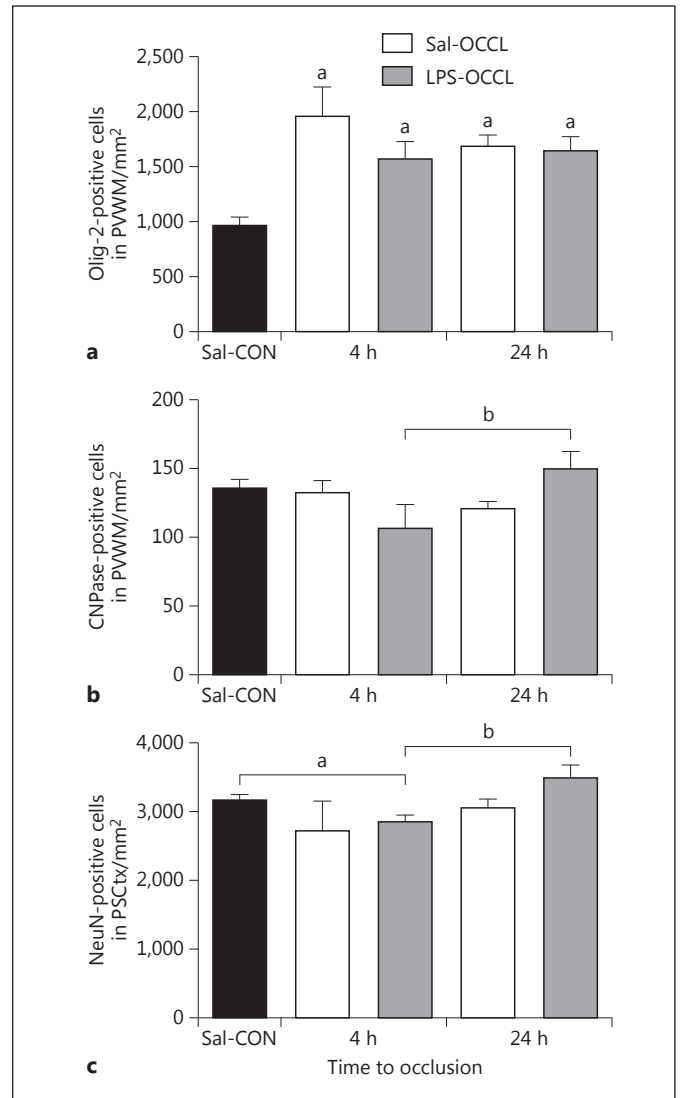


Fig. 5. Number of Olig-2- (a) and CNPase-positive (b) cells in the PVWM and those of NeuN-positive cells (c) in the parasagittal cortex (PSCtx). Cell numbers are presented as means \pm SEM. Saline sham occlusion control = Sal-CON ($n = 4$), occlusion 4 h after saline = 4 h Sal-OCCL ($n = 3$), occlusion 4 h after LPS = 4 h LPS-OCCL ($n = 6$), occlusion 24 h after saline = 24 h Sal-OCCL ($n = 4$), occlusion 24 h after LPS = 24 h LPS-OCCL ($n = 6$). Significance is shown as $p < 0.05$. ^a $p < 0.05$: significant difference from Sal-CON; ^b $p < 0.05$: significant difference between other groups.

tential clinical relevance since it is widely speculated that subclinical infection and HI may act in concert to exacerbate preterm brain injury [14, 17, 56–60].

In absolute numbers, acute severe HI, as used in the present study, is less common than chronic prenatal hypoxia [12]. Nevertheless, the incidence of acute perinatal hypoxia in preterm infants is reported to be much

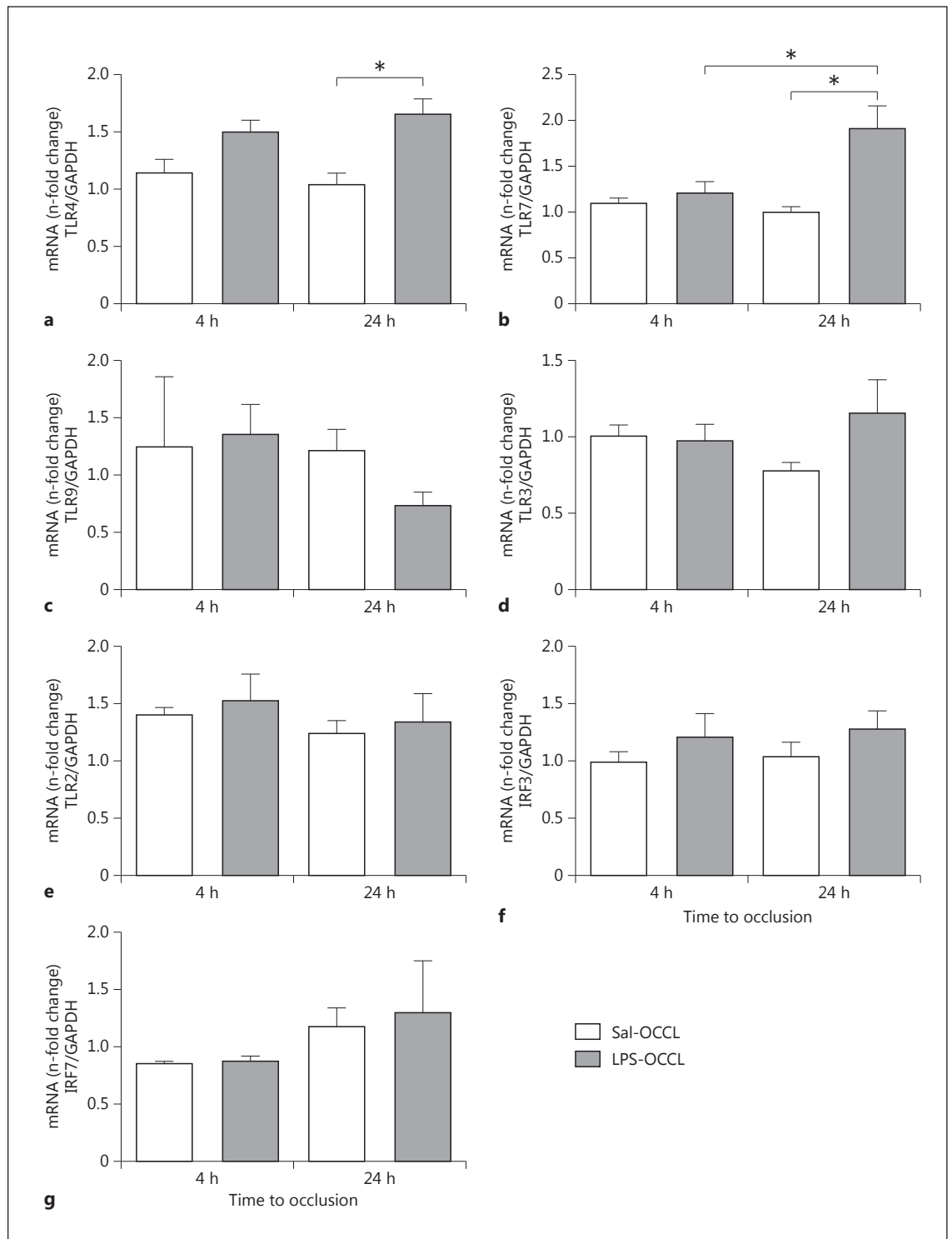


Fig. 6. mRNA expression of TLR4 (a), TLR7 (b), TLR9 (c), TLR3 (d), TLR2 (e), IRF3 (f) and IRF7 (g) in the preterm ovine fetal brain following LPS exposure and HI injury. Occlusion 4 h after saline = 4 h Sal-OCCL (n = 3), occlusion 4 h after LPS = 4 h LPS-

OCCL (n = 6), occlusion 24 h after saline = 24 h Sal-OCCL (n = 4), occlusion 24 h after LPS = 24 h LPS-OCCL (n = 6). Data are normalized to housekeeping gene GAPDH, and values are expressed as means \pm SEM. Significance is shown as * $p < 0.05$.

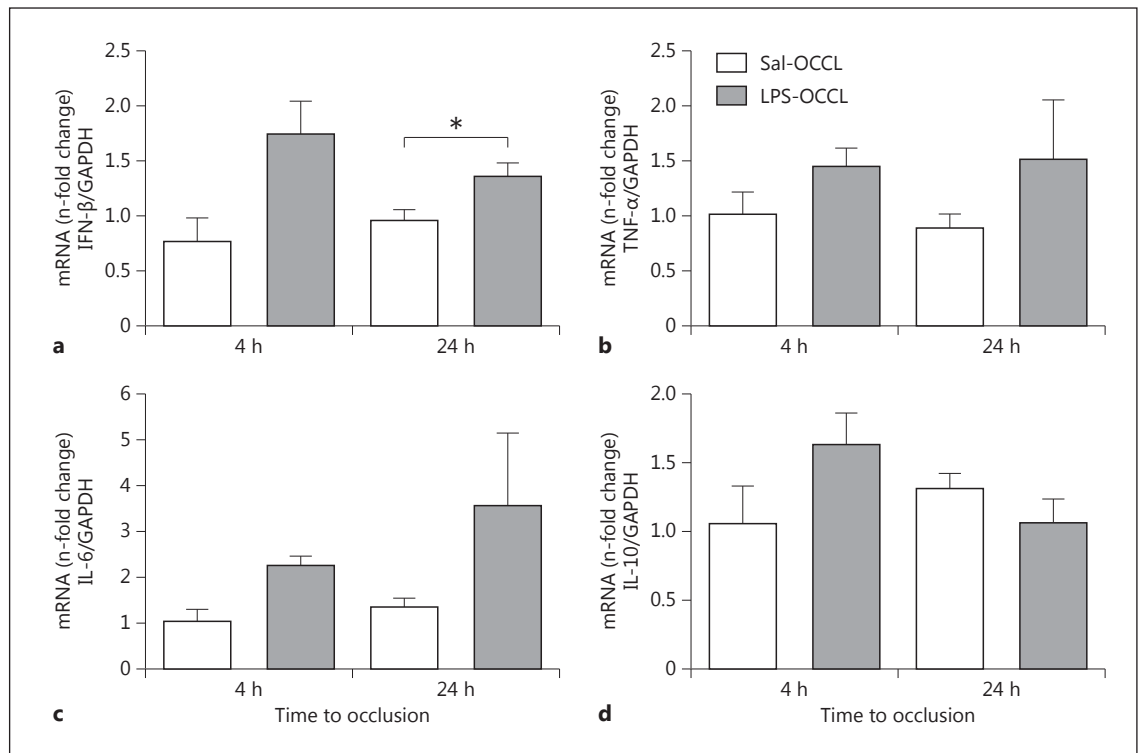


Fig. 7. mRNA expression of IFN- β (a), TNF- α (b), IL-6 (c) and IL-10 (d) in the preterm ovine fetal brain following LPS exposure and HI injury. Occlusion 4 h after saline = 4 h Sal-OCCL (n = 3), occlusion 4 h after LPS = 4 h LPS-OCCL (n = 6), occlusion 24 h after

saline = 24 h Sal-OCCL (n = 4), occlusion 24 h after LPS = 24 h LPS-OCCL (n = 6). Data are normalized to housekeeping gene GAPDH (a) or 18S (b-d), and values are expressed as means \pm SEM. Significance is shown as * $p < 0.05$.

greater than at term and, in turn, is associated with a very high risk of PVWM damage and neurodevelopmental disability [61, 62]. In the present study, moderate cerebral hypoperfusion induced by a 22-min period of bilateral carotid artery occlusion was associated with induction of both activated microglia and reactive astrocytes and apoptosis within the PVWM, consistent with previous studies in this paradigm [42, 63]. Further, hypoperfusion was associated with a significant increase in total (Olig-2-positive) oligodendrocytes 5 days after ischemia compared to saline controls, consistent with previous findings in the neonatal rat and fetal sheep [64, 65] that acute HI stimulates proliferation of oligodendrocyte progenitor cells. In contrast, fetuses exposed to ischemia 24 h but not 4 h after the last bolus of LPS showed marked attenuation of microglial induction, astrogliosis and apoptosis within the PVWM compared with ischemia alone. The present finding of a time-dependent effect of exposure to LPS and subsequent ischemia on the outcome of injury is highly consistent with studies of single acute doses of LPS in neonatal rats [13, 18, 24, 66]. However, our finding that

the severity of injury is not increased when ischemia is induced only 4 h after exposure to LPS is in contrast to the finding of sensitization to HI injury in the neonatal rat [18]. This difference is likely to reflect the repeated LPS exposure in the present study resulting in some degree of self-tolerance and cross-tolerance, as observed in a variety of models of brain injury [67].

Interestingly, the lack of effect with ischemia 4 h after LPS is in contrast to our previous findings demonstrating reduced microglial activation and astrogliosis with acute or chronic administration of LPS before asphyxia induced by complete umbilical cord occlusion in preterm fetal sheep [68]. The reason for this difference is unknown but may reflect the use of asphyxia, or the much higher doses of repeated LPS (1,000 ng/bolus compared to 50/100 ng in the present study). Alternatively, it may be related to continuation of the chronic infusion after the acute asphyxial insult in the previous study. In the present study, we used a very low-dose, repeated noninjurious regime in order to produce a mild fetal immune response which was stopped 4 or 24 h before HI in order to mimic

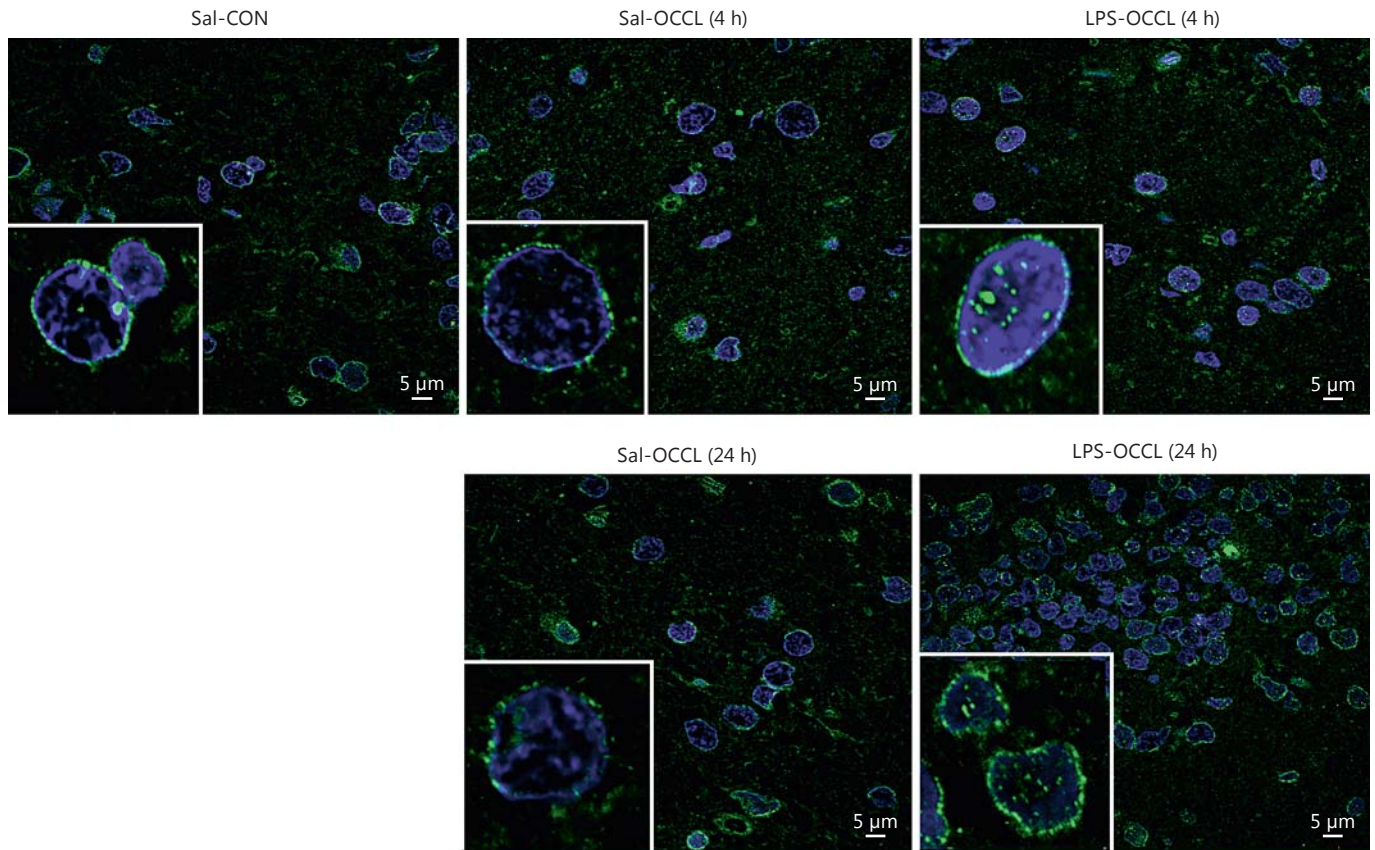


Fig. 8. Expression of TLR7 in the PVWM of preterm ovine fetal brains following LPS exposure and HI injury. Panels show representative immunofluorescent merged images of TLR7, detected with rabbit anti-TLR7 antibody (green) and DNA labeled with Hoechst 33258 (blue). Saline sham occlusion control = Sal-CON

(n = 4), occlusion 4 h after saline = 4 h Sal-OCCL (n = 3), occlusion 4 h after LPS = 4 h LPS-OCCL (n = 6), occlusion 24 h after saline = 24 h Sal-OCCL (n = 4), occlusion 24 h after LPS = 24 h LPS-OCCL (n = 6). **Insets** $\times 3$ magnification of a portion of each panel confirming staining of TLR7-positive cells. Magnification $\times 100$.

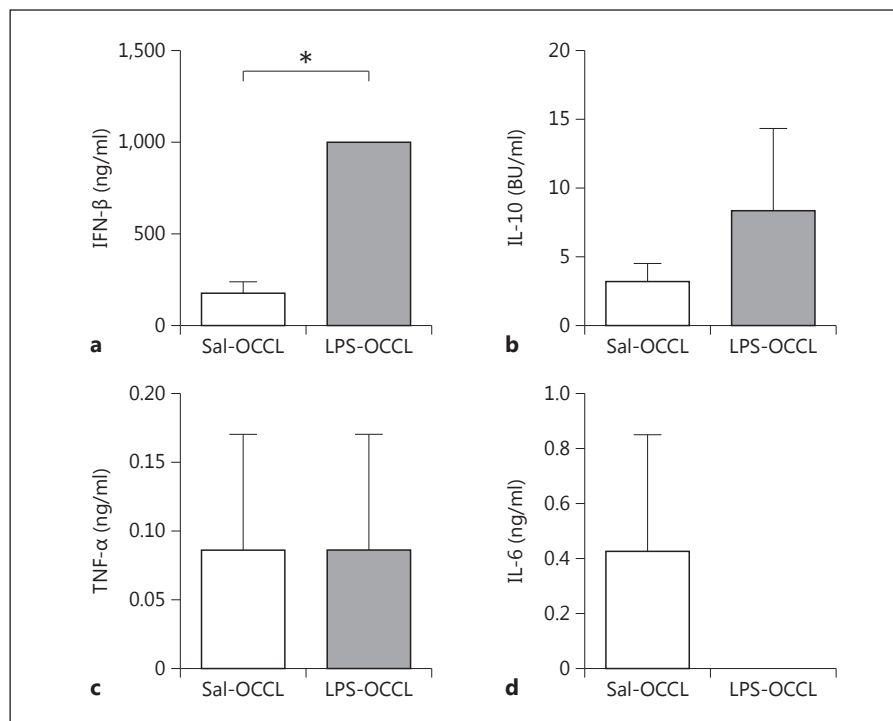
a state of intermittent systemic inflammation [20]. In future studies, it will be important to investigate whether continued or sustained exposure to low-dose LPS during induction of HI has any further effect on the evolution of injury. The present findings of delayed protection support the view that preconditioning or cross-tolerance induces a transient window of protection which is dependent on gene induction and de novo protein synthesis, consistent with *in vitro* [69, 70] and *in vivo* [71–75] neonatal and adult rat models of ischemia.

Although the molecular mechanisms that underlie preconditioning are unclear, it is generally accepted that immediate postischemic inflammation is a significant contributing factor to ischemic brain injury. Inflammation occurs through the action of proinflammatory cytokines such as TNF- α , IL-6 and IL-1 β . Production of these proinflammatory cytokines is initiated by signaling

through TLRs, in particular TLR4 [76], which recognize host-derived molecules released from injured tissue or cells as well as pathogen-associated molecular patterns which are present on neuronal, glial (microglia, astrocytes and oligodendrocytes) and endothelial cells [23]. Moreover, in adult stroke models TLR4 or TLR2 deficiency attenuates infarction [77, 78] indicating they play an important role in the pathogenesis of ischemic brain injury.

Reprogramming of this inflammatory response is thought to be a mechanism by which LPS, a potent TLR4 ligand, can induce protection against ischemia [22]. Our data showing a significant increase in TLR4 gene expression in association with an increase in both gene expression and circulating concentrations of the anti-inflammatory type 1 interferon IFN- β , in fetuses who were protected when exposed to ischemia 24 h following LPS,

Fig. 9. Concentrations of IFN- β (a), IL-10 (b), TNF- α (c) and IL-6 (d) in fetal plasma collected from 24 h Sal-OCCL (n = 4) and 24 h LPS-OCCL (n = 6) groups, 5 days after carotid occlusion. BU = Biological units. IFN- β concentrations in the 24 h LPS-OCCL group were above the calibration range, and values were defined as the upper limit of the range (1,000 pg/ml). IL-6 concentrations were all below the level of detection (0.097 ng/ml) for the 24 h LPS-OCCL group. Data are presented as means \pm SEM. Significance is shown as * $p < 0.05$.



suggest that TLR4 signaling is redirected via the TLR4 adapter molecule TRIF (TIR domain-containing adaptor protein inducing IFN- β). IFN- β is reported to be neuroprotective against ischemia in adult models and is believed to be involved in the regulation of TLRs [79]. Further, TRIF-deficient mice do not show reduced infarction or improvement in neurological deficits following ischemia indicating that the TRIF signaling pathway may be required for protection [80]. Thus, enhanced TLR4 signaling to TRIF-IFN- β could potentially contribute to neuroprotection. A limitation of the present study is that gene expression and IFN- β protein changes were not assessed before ischemia (i.e. at 4 and 24 h) or with LPS alone; further studies will be needed to evaluate the time course and drivers of fetal inflammation fully.

Our findings are consistent with studies in an adult mouse stroke model showing that LPS-induced protection occurs via induction of IFN- β and interferon-stimulated genes through TRIF, mediated by the IRF3 [27]. Paradoxically, in an elegant series of studies by the same group, genomic profiles of mice preconditioned with the TLR ligands LPS and TLR9 (CpG) or brief ischemia, induction of IRF7 (an inducible IRF, which is thought to be involved in positive regulation of type I induction [81]) but not IRF3 gene expression were demonstrated for all preconditioning paradigms [28]. Importantly, they also

showed that mice deficient in either IRF3 or IRF7 did not develop preconditioning after LPS [27]. Given this, we undertook an examination of both IRF3 and IRF7 gene expression and found neither to be significantly changed. However, gene expression was determined 5 days after injury, so it is possible that any change was missed. Alternatively, it is possible that there could be increased nuclear localization of these transcription factors to regulate transcription of IFN- β , as shown in adult mice [27].

Unlike TLR4 which signals through the TRIF pathway, TLR7 and TLR9 signaling occur preferentially through MyD88 and can stimulate production of type I IFNs [82]. In the present study, we observed a robust increase in TLR7 mRNA expression, but not TLR9, occurring in association with an increase in IFN- β expression in those fetuses exhibiting neuroprotection when ischemia was induced 24 h after LPS. Furthermore, immunofluorescence staining suggested substantially greater intensity of TLR7-immunopositive cells within the PVWM. Unfortunately, we were unable to identify the specific cell type, due to technical difficulties. Nevertheless, this suggests TLR7 activation may potentially play a role in LPS-induced neuroprotection. In addition, TLR7 is a more effective inducer of type I IFNs (IFN- α and IFN- β) than TLR4 or TLR9 [83]; thus, LPS-induced neuroprotection in the developing brain may rely on activation of TLR7

and subsequent MyD88-dependent type I IFN production. Consistent with this speculation, recent findings by Leung et al. [34] support neuroprotection with the TLR7 ligand gardiquimod in an adult mouse stroke model.

Production of type I IFNs by TLR7 signaling is mediated by IRF7, but not IRF3 [84, 85]. Whereas we were unable to demonstrate induction of IRF7, Leung et al. [34] observed that TLR7-induced neuroprotection occurred in association with an increase in circulating concentrations of IFN- α but not IFN- β . This is in contrast to our present findings of a significantly higher plasma concentration of IFN- β , 5 days after ischemia in those fetuses in which ischemia was induced 24 h after LPS. Moreover, they observed that in IRF7- and TNF-deficient mice preconditioned with gardiquimod, TLR7-induced neuroprotection was dependent on IRF7-mediated induction of systemic levels of IFN- α but independent of TNF- α .

In contrast to previous findings that TNF- α is required to establish LPS-induced preconditioning [33], we did not find a significant increase in TNF- α gene expression with LPS preconditioning. Potentially, this could reflect the relatively long time course of the present study, and that there was transient cerebral expression after ischemia. Further, we recognize that mRNA expression and protein levels can be discordant. A limitation of the present study is that plasma samples were not available at all time points for measurement of circulating cytokines. However, it is notable that 5 days following ischemia, circulating concentrations of IFN- β in the 24 h LPS-OCCL group were above the calibration range of the assay, whereas no difference was observed for other cytokines raising the possibility that upregulation of cerebral and

peripheral IFN- β may potentially be a critical feature of LPS preconditioning.

In summary, this is the first demonstration that LPS preconditioning 24 h before HI in the preterm fetal sheep is associated with an altered TLR response to HI. Furthermore, the neuroprotective effect of LPS preconditioning is associated with a novel pattern of TLR mRNA expression, whereby LPS preconditioning induces a robust increase in both TLR4 and TLR7 in association with an increase in the neuroprotective type I IFN IFN- β . Although these data cannot definitively demonstrate a causal relationship, they suggest that TLR4 and/or TLR7 may contribute to inducing expression of IFN- β and raise the intriguing possibility that IFN- β may mediate the neuroprotective effect of LPS preconditioning. Future studies are required to determine whether the increase in IFN- β is causally involved in endogenous protection of the preterm brain.

Acknowledgments

This work was supported by grants from the Health Research Council of New Zealand, Cure Kids, and Gravidia: National Centre for Growth and Development, a Centre of Research Excellence administered by the New Zealand Tertiary Education Commission.

Disclosure Statement

The authors have neither financial relationships relevant to this article nor conflicts of interest to disclose. No honorarium, grant or other form of payment was given to anyone to produce this study.

References

- 1 Committee on Understanding Premature Birth and Assuring Healthy Outcomes; in Behrman RE, Butler AS (eds): Preterm Birth: Causes, Consequences, and Prevention. Washington, Institute of Medicine of the National Academies, 2007, <http://books.nap.edu/catalog/11622.html#toc>.
- 2 Shatrov JG, Birch SC, Lam LT, Quinlivan JA, McIntyre S, Mendz GL: Chorioamnionitis and cerebral palsy: a meta-analysis. *Obstet Gynecol* 2010;116:387–392.
- 3 Hatfield T, Wing DA, Buss C, Head K, Muf-tuler LT, Davis EP: Magnetic resonance imaging demonstrates long-term changes in brain structure in children born preterm and exposed to chorioamnionitis. *Am J Obstet Gynecol* 2011;205:027.
- 4 Dean JM, Shi Z, Fleiss B, Gunn KC, Groenendaal F, van Bel F, Derrick M, Juul SE, Tan S, Gressens P, Mallard C, Bennet L, Gunn AJ: A Critical Review of Models of Perinatal Infection. *Dev Neurosci* 2015;37:289–304.
- 5 Farrelly L, Focking M, Piontkewitz Y, Dicker P, English J, Wynne K, Cannon M, Cagney G, Cotter DR: Maternal immune activation induces changes in myelin and metabolic proteins, some of which can be prevented with risperidone in adolescence. *Dev Neurosci* 2015;37:43–55.
- 6 Li WY, Chang YC, Lee LJ: Prenatal infection affects the neuronal architecture and cognitive function in adult mice. *Dev Neurosci* 2014;36:359–370.
- 7 Balakrishnan B, Dai H, Janisse J, Romero R, Kannan S: Maternal endotoxin exposure results in abnormal neuronal architecture in the newborn rabbit. *Dev Neurosci* 2013;35:396–405.
- 8 Rousset CI, Kassem J, Aubert A, Planchenault D, Gressens P, Chalon S, Belzung C, Saliba E: Maternal exposure to lipopolysaccharide leads to transient motor dysfunction in neonatal rats. *Dev Neurosci* 2013;35:172–181.
- 9 Malaeb SN, Davis JM, Pinz IM, Newman JL, Dammann O, Rios M: Effect of sustained postnatal systemic inflammation on hippocampal volume and function in mice. *Pediatr Res* 2014;76:363–369.

- 10 Helderman JB, O'Shea TM, Kuban KC, Allred EN, Hecht JL, Dammann O, Paneth N, McElrath TF, Onderdonk A, Leviton A: Antenatal antecedents of cognitive impairment at 24 months in extremely low gestational age newborns. *Pediatrics* 2012;129:494–502.
- 11 O'Shea TM, Allred EN, Kuban KC, Dammann O, Paneth N, Fichorova R, Hirtz D, Leviton A: Elevated concentrations of inflammation-related proteins in postnatal blood predict severe developmental delay at 2 years of age in extremely preterm infants. *J Pediatr* 2012;160:395–401.
- 12 Leviton A, Fichorova RN, O'Shea TM, Kuban K, Paneth N, Dammann O, Allred EN: Two-hit model of brain damage in the very preterm newborn: small for gestational age and postnatal systemic inflammation. *Pediatr Res* 2013;73:362–370.
- 13 Lin HY, Huang CC, Chang KF: Lipopolysaccharide preconditioning reduces neuroinflammation against hypoxic-ischemia and provides long-term outcome of neuroprotection in neonatal rat. *Pediatr Res* 2009;66:254–259.
- 14 Eklind S, Mallard C, Leverin AL, Gilland E, Blomgren K, Mattsby-Baltzer I, Hagberg H: Bacterial endotoxin sensitizes the immature brain to hypoxic-ischaemic injury. *Eur J Neurosci* 2001;13:1101–1106.
- 15 Yang L, Sameshima H, Ikeda T, Ikenoue T: Lipopolysaccharide administration enhances hypoxic-ischemic brain damage in newborn rats. *J Obstet Gynaecol Res* 2004;30:142–147.
- 16 Ikeda T, Mishima K, Aoo N, Egashira N, Iwasaki K, Fujiwara M, Ikenoue T: Combination treatment of neonatal rats with hypoxia-ischemia and endotoxin induces long-lasting memory and learning impairment that is associated with extended cerebral damage. *Am J Obstet Gynecol* 2004;191:2132–2141.
- 17 Wang LW, Chang YC, Lin CY, Hong JS, Huang CC: Low-dose lipopolysaccharide selectively sensitizes hypoxic ischemia-induced white matter injury in the immature brain. *Pediatr Res* 2010;68:41–47.
- 18 Eklind S, Mallard C, Arvidsson P, Hagberg H: Lipopolysaccharide induces both a primary and a secondary phase of sensitization in the developing rat brain. *Pediatr Res* 2005;58:112–116.
- 19 Leviton A, Allred EN, Kuban KC, Hecht JL, Onderdonk AB, O'Shea TM, Paneth N: Microbiologic and histologic characteristics of the extremely preterm infant's placenta predict white matter damage and later cerebral palsy: the ELGAN study. *Pediatr Res* 2010;67:95–101.
- 20 Dammann O, Leviton A: Intermittent or sustained systemic inflammation and the preterm brain. *Pediatr Res* 2014;75:376–380.
- 21 Stoll BJ, Hansen NI, Adams-Chapman I, Fanaroff AA, Hintz SR, Vohr B, Higgins RD: Neurodevelopmental and growth impairment among extremely low-birth-weight infants with neonatal infection. *JAMA* 2004;292:2357–2365.
- 22 Marsh BJ, Williams-Karnesky RL, Stenzel-Poore MP: Toll-like receptor signaling in endogenous neuroprotection and stroke. *Neuroscience* 2009;158:1007–1020.
- 23 Hanke ML, Kielian T: Toll-like receptors in health and disease in the brain: mechanisms and therapeutic potential. *Clin Sci (Lond)* 2011;121:367–387.
- 24 Hickey E, Shi H, Van Arsdell G, Askalan R: Lipopolysaccharide-induced preconditioning against ischemic injury is associated with changes in Toll-like receptor 4 expression in the rat developing brain. *Pediatr Res* 2011;70:10–14.
- 25 Mallard C, Wang X, Hagberg H: The role of Toll-like receptors in perinatal brain injury. *Clin Perinatol* 2009;36:763–772, v–vi.
- 26 Mallard C, Wang X: Infection-induced vulnerability of perinatal brain injury. *Neurol Res Int* 2012;2012:102153.
- 27 Marsh B, Stevens SL, Packard AE, Gopalan B, Hunter B, Leung PY, Harrington CA, Stenzel-Poore MP: Systemic lipopolysaccharide protects the brain from ischemic injury by reprogramming the response of the brain to stroke: a critical role for IRF3. *J Neurosci* 2009;29:9839–9849.
- 28 Stevens SL, Leung PY, Vartanian KB, Gopalan B, Yang T, Simon RP, Stenzel-Poore MP: Multiple preconditioning paradigms converge on interferon regulatory factor-dependent signaling to promote tolerance to ischemic brain injury. *J Neurosci* 2011;31:8456–8463.
- 29 Kariko K, Weissman D, Welsh FA: Inhibition of Toll-like receptor and cytokine signaling – a unifying theme in ischemic tolerance. *J Cereb Blood Flow Metab* 2004;24:1288–1304.
- 30 Stenzel-Poore MP, Stevens SL, King JS, Simon RP: Preconditioning reprograms the response to ischemic injury and primes the emergence of unique endogenous neuroprotective phenotypes: a speculative synthesis. *Stroke* 2007;38:680–685.
- 31 Pradillo JM, Fernandez-Lopez D, Garcia-Yebenes I, Sobrado M, Hurtado O, Moro MA, Lizasoain I: Toll-like receptor 4 is involved in neuroprotection afforded by ischemic preconditioning. *J Neurochem* 2009;109:287–294.
- 32 Stevens SL, Ciesielski TM, Marsh BJ, Yang T, Homen DS, Boule JL, Lessov NS, Simon RP, Stenzel-Poore MP: Toll-like receptor 9: a new target of ischemic preconditioning in the brain. *J Cereb Blood Flow Metab* 2008;28:1040–1047.
- 33 Rosenzweig HL, Minami M, Lessov NS, Coste SC, Stevens SL, Henshall DC, Meller R, Simon RP, Stenzel-Poore MP: Endotoxin preconditioning protects against the cytotoxic effects of TNFalpha after stroke: a novel role for TNFalpha in LPS-ischemic tolerance. *J Cereb Blood Flow Metab* 2007;27:1663–1674.
- 34 Leung PY, Stevens SL, Packard AE, Lessov NS, Yang T, Conrad VK, van den Dungen NN, Simon RP, Stenzel-Poore MP: Toll-like receptor 7 preconditioning induces robust neuroprotection against stroke by a novel type I interferon-mediated mechanism. *Stroke* 2012;43:1383–1389.
- 35 Kaul D, Habel P, Derkow K, Kruger C, Franzoni E, Wulczyn FG, Bereswill S, Nitsch R, Schott E, Veh R, Naumann T, Lehnardt S: Expression of Toll-like receptors in the developing brain. *PLoS One* 2012;7:e37767.
- 36 McIntosh GH, Baghurst KI, Potter BJ, Hetzel BS: Foetal brain development in the sheep. *Neuropathol Appl Neurobiol* 1979;5:103–114.
- 37 Tsuji M, Saul JP, du Plessis A, Eichenwald E, Sobh J, Crocker R, Volpe JJ: Cerebral intravascular oxygenation correlates with mean arterial pressure in critically ill premature infants. *Pediatrics* 2000;106:625–632.
- 38 Greisen G: To autoregulate or not to autoregulate – that is no longer the question. *Semin Perinatol* 2009;16:207–215.
- 39 Soul JS, Hammer PE, Tsuji M, Saul JP, Bassan H, Limperopoulos C, Disalvo DN, Moore M, Akins P, Ringer S, Volpe JJ, Trachtenberg F, du Plessis AJ: Fluctuating pressure-passivity is common in the cerebral circulation of sick premature infants. *Pediatr Res* 2007;61:467–473.
- 40 Khwaja O, Volpe JJ: Pathogenesis of cerebral white matter injury of prematurity. *Arch Dis Child Fetal Neonatal Ed* 2008;93:F153–F161.
- 41 Davidson JO, Yuill CA, Wassink G, Bennet L, Gunn AJ: Spontaneous pre-existing hypoxia does not affect brain damage after global cerebral ischaemia in late-gestation fetal sheep. *Dev Neurosci* 2015;37:56–65.
- 42 Fraser M, Bennet L, Gunning M, Williams C, Gluckman PD, George S, Gunn AJ: Cortical electroencephalogram suppression is associated with post-ischemic cortical injury in 0.65 gestation fetal sheep. *Brain Res Dev Brain Res* 2005;154:45–55.
- 43 Fraser M, Bennet L, Helliwell R, Wells S, Williams C, Gluckman P, Gunn AJ, Inder T: Regional specificity of magnetic resonance imaging and histopathology following cerebral ischemia in preterm fetal sheep. *Reprod Sci* 2007;14:182–191.
- 44 Plaisier A, Govaert P, Lequin MH, Dudink J: Optimal timing of cerebral MRI in preterm infants to predict long-term neurodevelopmental outcome: a systematic review. *AJNR Am J Neuroradiol* 2014;35:841–847.
- 45 Inder TE, Wells SJ, Mogridge NB, Spencer C, Volpe JJ: Defining the nature of the cerebral abnormalities in the premature infant: a qualitative magnetic resonance imaging study. *J Pediatr* 2003;143:171–179.
- 46 Counsell SJ, Allsop JM, Harrison MC, Larkman DJ, Kennea NL, Kapellou O, Cowan FM, Hajnal JV, Edwards AD, Rutherford MA: Diffusion-weighted imaging of the brain in preterm infants with focal and diffuse white matter abnormality. *Pediatrics* 2003;112:1–7.
- 47 Miller SP, Ferriero DM, Leonard C, Piecuch R, Glidden DV, Partridge JC, Perez M, Mukherjee P, Vigneron DB, Barkovich AJ: Early brain injury in premature newborns detected with magnetic resonance imaging is associated with adverse early neurodevelopmental outcome. *J Pediatr* 2005;147:609–616.

- 48 Jakovcevski I, Filipovic R, Mo Z, Rakic S, Zecevic N: Oligodendrocyte development and the onset of myelination in the human fetal brain. *Front Neuroanat* 2009;3:5.
- 49 Ramakers C, Ruijter JM, Deprez RH, Moorman AF: Assumption-free analysis of quantitative real-time polymerase chain reaction (PCR) data. *Neurosci Lett* 2003;339:62–66.
- 50 Pfaffl MW, Tichopad A, Prgomet C, Neuvians TP: Determination of stable housekeeping genes, differentially regulated target genes and sample integrity: BestKeeper – Excel-based tool using pair-wise correlations. *Biotechnol Lett* 2004;26:509–515.
- 51 Weaver-Mikaere L, Gunn AJ, Mitchell MD, Bennet L, Fraser M: LPS and TNF alpha modulate AMPA/NMDA receptor subunit expression and induce PGE2 and glutamate release in preterm fetal ovine mixed glial cultures. *J Neuroinflamm* 2013;10:153.
- 52 Weaver-Mikaere L, Gunn AJ, Bennet L, Mitchell MD, Fraser M: Inhibition of matrix metalloproteinases-2/-9 transiently reduces pre-oligodendrocyte loss during lipopolysaccharide but not tumour necrosis factor-alpha-induced inflammation in fetal ovine glial culture. *Dev Neurosci* 2013;35:461–473.
- 53 Livak KJ, Schmittgen TD: Analysis of relative gene expression data using real-time quantitative PCR and the $2^{-\Delta\Delta C(T)}$ method. *Methods* 2001;25:402–408.
- 54 Kwong LS, Hope JC, Thom ML, Sopp P, Duggan S, Bembridge GP, Howard CJ: Development of an ELISA for bovine IL-10. *Vet Immunol Immunopathol* 2002;85:213–223.
- 55 Wattegedera S, Rocchi M, Sales J, Howard CJ, Hope JC, Entrican G: Antigen-specific peripheral immune responses are unaltered during normal pregnancy in sheep. *J Reprod Immunol* 2008;77:171–178.
- 56 Yanowitz TD, Jordan JA, Gilmour CH, Towbin R, Bowen A, Roberts JM, Brozanski BS: Hemodynamic disturbances in premature infants born after chorioamnionitis: association with cord blood cytokine concentrations. *Pediatr Res* 2002;51:310–316.
- 57 Kaukola T, Herva R, Perhomaa M, Paakko E, Kingsmore S, Vainionpaa L, Hallman M: Population cohort associating chorioamnionitis, cord inflammatory cytokines and neurologic outcome in very preterm, extremely low birth weight infants. *Pediatr Res* 2006;59:478–483.
- 58 Wang X, Hagberg H, Nie C, Zhu C, Ikeda T, Mallard C: Dual role of intrauterine immune challenge on neonatal and adult brain vulnerability to hypoxia-ischemia. *J Neuropathol Exp Neurol* 2007;66:552–561.
- 59 Girard S, Kadhim H, Beaudet N, Sarret P, Sebire G: Developmental motor deficits induced by combined fetal exposure to lipopolysaccharide and early neonatal hypoxia/ischemia: a novel animal model for cerebral palsy in very premature infants. *Neuroscience* 2009;158:673–682.
- 60 Fukuda S, Yokoi K, Kitajima K, Tsunoda Y, Hayashi N, Shimizu S, Yoshida T, Hamajima N, Watanabe I, Goto H: Influence of premature rupture of membrane on the cerebral blood flow in low-birth-weight infant after the delivery. *Brain Dev* 2010;32:631–635.
- 61 Low JA, Froese AF, Galbraith RS, Sauerbrei EE, McKinven JP, Karchmar EJ: The association of fetal and newborn metabolic acidosis with severe periventricular leukomalacia in the preterm newborn. *Am J Obstet Gynecol* 1990;162:977–981, discussion 981–972.
- 62 Low JA, Galbraith RS, Muir DW, Killen HL, Pater EA, Karchmar EJ: Mortality and morbidity after intrapartum asphyxia in the preterm fetus. *Obstet Gynecol* 1992;80:57–61.
- 63 Riddle A, Luo NL, Manese M, Beardsley DJ, Green L, Rorvik DA, Kelly KA, Barlow CH, Kelly JJ, Hohimer AR, Back SA: Spatial heterogeneity in oligodendrocyte lineage maturation and not cerebral blood flow predicts fetal ovine periventricular white matter injury. *J Neurosci* 2006;26:3045–3055.
- 64 Riddle A, Dean J, Buser JR, Gong X, Maire J, Chen K, Ahmad T, Cai V, Nguyen T, Kroenke CD, Hohimer AR, Back SA: Histopathological correlates of magnetic resonance imaging-defined chronic perinatal white matter injury. *Ann Neurol* 2011;70:493–507.
- 65 Segovia KN, McClure M, Moravec M, Luo NL, Wan Y, Gong X, Riddle A, Craig A, Struve J, Sherman LS, Back SA: Arrested oligodendrocyte lineage maturation in chronic perinatal white matter injury. *Ann Neurol* 2008;63:520–530.
- 66 Eklind S, Hagberg H, Wang X, Savman K, Leverin AL, Hedtjarn M, Mallard C: Effect of lipopolysaccharide on global gene expression in the immature rat brain. *Pediatr Res* 2006;60:161–168.
- 67 Stetler RA, Leak RK, Gan Y, Li P, Zhang F, Hu X, Jing Z, Chen J, Zigmond MJ, Gao Y: Preconditioning provides neuroprotection in models of CNS disease: paradigms and clinical significance. *Prog Neurobiol* 2014;114:58–83.
- 68 Van den Heuvel LG, Mathai S, Davidson JO, Lear CA, Booth LC, Fraser M, Gunn AJ, Bennet L: Synergistic white matter protection with acute-on-chronic endotoxin and subsequent asphyxia in preterm fetal sheep. *J Neuroinflamm* 2014;11:89.
- 69 Gage AT, Stanton PK: Hypoxia triggers neuroprotective alterations in hippocampal gene expression via a heme-containing sensor. *Brain Res* 1996;719:172–178.
- 70 Wick A, Wick W, Waltenberger J, Weller M, Dichgans J, Schulz JB: Neuroprotection by hypoxic preconditioning requires sequential activation of vascular endothelial growth factor receptor and Akt. *J Neurosci* 2002;22:6401–6407.
- 71 Currie RW, Ellison JA, White RF, Feuerstein GZ, Wang X, Barone FC: Benign focal ischemic preconditioning induces neuronal Hsp70 and prolonged astroglialosis with expression of Hsp27. *Brain Res* 2000;863:169–181.
- 72 Nishio S, Yunoki M, Chen ZF, Anzivino MJ, Lee KS: Ischemic tolerance in the rat neocortex following hypothermic preconditioning. *J Neurosurg* 2000;93:845–851.
- 73 Bordet R, Deplanque D, Maboudou P, Pui-sieux F, Pu Q, Robin E, Martin A, Bastide M, Leys D, Lhermitte M, Dupuis B: Increase in endogenous brain superoxide dismutase as a potential mechanism of lipopolysaccharide-induced brain ischemic tolerance. *J Cereb Blood Flow Metab* 2000;20:1190–1196.
- 74 Barone FC, White RF, Spera PA, Ellison J, Currie RW, Wang X, Feuerstein GZ: Ischemic preconditioning and brain tolerance: temporal histological and functional outcomes, protein synthesis requirement, and interleukin-1 receptor antagonist and early gene expression. *Stroke* 1998;29:1937–1950.
- 75 Lin HY, Wu CL, Huang CC: The Akt-endothelial nitric oxide synthase pathway in lipopolysaccharide preconditioning-induced hypoxic-ischemic tolerance in the neonatal rat brain. *Stroke* 2010;41:1543–1551.
- 76 Gao Y, Fang X, Tong Y, Liu Y, Zhang B: TLR4-mediated MyD88-dependent signaling pathway is activated by cerebral ischemia-reperfusion in cortex in mice. *Biomed Pharmacother* 2009;63:442–450.
- 77 Cao CX, Yang QW, Lv FL, Cui J, Fu HB, Wang JZ: Reduced cerebral ischemia-reperfusion injury in Toll-like receptor 4 deficient mice. *Biochem Biophys Res Commun* 2007;353:509–514.
- 78 Ziegler G, Harhausen D, Schepers C, Hoffmann O, Rohr C, Prinz V, Konig J, Lehrach H, Niefeld W, Trendelenburg G: TLR2 has a detrimental role in mouse transient focal cerebral ischemia. *Biochem Biophys Res Commun* 2007;359:574–579.
- 79 Veldhuis WB, Derksen JW, Floris S, Van Der Meide PH, De Vries HE, Schepers J, Vos IM, Dijkstra CD, Kappelle LJ, Nicolay K, Bar PR: Interferon-beta blocks infiltration of inflammatory cells and reduces infarct volume after ischemic stroke in the rat. *J Cereb Blood Flow Metab* 2003;23:1029–1039.
- 80 Hua F, Wang J, Sayeed I, Ishrat T, Atif F, Stein DG: The TRIF-dependent signaling pathway is not required for acute cerebral ischemia/reperfusion injury in mice. *Biochem Biophys Res Commun* 2009;390:678–683.
- 81 Honda K, Takaoka A, Taniguchi T: Type I interferon gene induction by the interferon regulatory factor family of transcription factors. *Immunity* 2006;25:349–360.
- 82 Mogensen TH: Pathogen recognition and inflammatory signaling in innate immune defenses. *Clin Microbiol Rev* 2009;22:240–273.
- 83 Longhi MP, Trumpfeller C, Idoyaga J, Caskey M, Matos I, Kluger C, Salazar AM, Colonna M, Steinman RM: Dendritic cells require a systemic type I interferon response to mature and induce CD4+ Th1 immunity with poly IC as adjuvant. *J Exp Med* 2009;206:1589–1602.
- 84 Kawai T, Akira S: TLR signaling. *Semin Immunol* 2007;19:24–32.
- 85 Honda K, Yanai H, Negishi H, Asagiri M, Sato M, Mizutani T, Shimada N, Ohba Y, Takaoka A, Yoshida N, Taniguchi T: IRF-7 is the master regulator of type-I interferon-dependent immune responses. *Nature* 2005;434:772–777.

Reproduced with permission of the copyright owner. Further reproduction prohibited without permission.